Preprints of the
9th International Symposium on Advanced Control of Chemical Processes
The International Federation of Automatic Control
June 7-10, 2015, Whistler, British Columbia, Canada

Model-based control to maximise biomass and PHB in the autotrophic cultivation of *Ralstonia eutropha* ⋆

Flavia Neddermeyer * **Niko Rossner** ** **Rudibert King** *

* *Chair of Measurement and Control, Technische Universität Berlin, Secr. ER 2-1, Hardenbergstraße 36a, 10623 Berlin, Germany(e-mail: flavia.neddermeyer@tu-berlin.de, and rudibert.king@tu-berlin.de).*
** *Present address: Bayer Technology Services GmbH, Process Dynamics and Operation, Kaiser-Wilhelm-Allee 60, 51368 Leverkusen, Germany (e-mail: niko.rossner@bayer.com).*

Abstract: This paper presents a realisation of a closed-loop controlled autotrophic fed-batch cultivation of *Ralstonia eutropha* H16 with the aim to maximise the amount of biomass and internal storage compound PHB. The specific control unit is a model-based on-line trajectory planning with a sigma-point Kalman filter for state estimation and an additional gas phase controller. For the control, a medium-sized structured model describing the process is proposed and compared to cultivation data. The model considers the internal storage of PHB by *R. eutropha* and pays special attention to the production of the oxygen-tolerant membrane-bound hydrogenase. This enzyme is in the center of biological research as a component of a biological fuel cell. It is shown that on-line optimisation works for maximising the amounts of biomass and PHB.

Keywords: Ralstonia eutropha, model-based control, sigma-point Kalman filter, on-line trajectory planning, optimisation, closed-loop, autotrophic cultivation, fed-batch.

1. INTRODUCTION

Model-based control has become a powerful tool for running processes optimally. In biotechnology, control is applied with the main goal to improve the product yield and quality. Besides basic, standard controllers, e.g., to adjust the pH, the idea is to control the process additionally on a more general level by means of, e.g., model-based control. This has been investigated in the past years by various groups. Some studies on and industrial solutions for advanced bioprocess control of specific bioprocesses are collected in Mandenius and Titchener-Hooker (2013). One of the first experimental verification of model predictive control with a complex nonlinear model of a biological process has been presented in Waldraff et al. (1993), see as well Waldraff et al. (1997) or King (1997). In this work, on-line trajectory planning (TP) is realised by calculating the best reference values for an underlying gas-controller and optimal feeding profiles for other substrates. This scheme makes the process more efficient compared to those that are run manually by changing reference values according to experience. Besides a higher product yield, an automated model-based closed-loop control leads to an increased reproducibility as well.

This work deals with the model-based on-line TP of the autotrophic cultivation of *Ralstonia eutropha (R. e.)*. Autotrophic means that the organism grows on inorganic substrates, without, e.g., sugars as a source of energy and carbon. In the autotrophic mode, growth and productivity of *R. e.* depend on the concentrations of the substrates ammonium and phosphate as well as the dissolved gas concentrations of hydrogen, oxygen and carbon dioxide. The latter one serves as a carbon source and is assimilated. Hydrogen is the energy source for the organism and is oxidised to water.

During the cultivation, the states which are non-measurable, e.g., the amount of biomass, product and substrates, are estimated with a sigma-point Kalman filter (SPKF) described in Rossner (2014). The SPKF estimates the most probable values for the states by taking the on-line and at-line measurements of the process and the simulation results into account. These estimated states are assembled in a state vector and form the start values for an on-line optimisation. In the optimisation, the needed feeding trajectories with the aim to maximise biomass and PHB are calculated.

Applying model-based control for the autotrophic cultivation of *R. e.* requires a model of the process which is as simple as possible to make the on-line calculations tractable in a real-time environment. At the same time it has to incorporate all relevant quantities and dynamics so that the process is well described and the on-line TP works. As three substrates are primarily of gaseous nature and the dissolved gas concentrations depend on the gas composition in the headspace of the fermenter, the model has to describe both the gaseous and the liquid phase.

The paper is structured as follows: The materials and methods for the autotrophic cultivation are listed in section 2. Then, in section 3, the applied control system for

⋆ This work was supported by the DFG in the framework of the cluster of excellence UniCat.

the process is described. This is followed by the introduction of the process model in section 4. Two parameter identification experiments are shown, compared to the simulation results and the identified parameters are listed. In section 5, the results of a cultivation that ran with a closed-loop model-based control are shown and discussed. Finally, some conclusive remarks are drawn in section 6.

2. MATERIALS AND METHODS

The strain used was *Ralstonia eutropha* (H16). The feeding compositions are given in Tab. 1. The cultivation was started with 10.5 L defined medium.

Table 1. Feedings composition for *R. e.*

Feeding	Chemical	Conc. [g·L^{-1}]
Phosphate (P)	Na_2HPO_4 ($2H_2O$)	39.16
	KH_2PO_4	13.03
Ammonium (N)	NH_4Cl	296.94
Iron and	$MgSO_4$ ($7H_2O$)	20
trace elements	$CaCl_2$ ($2H_2O$)	1.00
	$FeCl_3$ ($6H_2O$)	1.00
	$NiCl_2$ ($6H_2O$)	0.024
	$ZnSO_4$ ($7H_2O$)	0.01
	$MnCl_2$ ($2H_2O$)	0.003
	H_3BO_3	0.03
	$CuCl_2$ ($2H_2O$)	0.001
	Na_2MoO_4 ($2H_2O$)	0.003
	$CoCl_2$ ($6H_2O$)	0.02

The initial medium concentrations of iron and trace elements were 1/100 of those in the feeding. Ammonium concentration was 1/5 of the feeding and phosphate either 1/10 or 1/30 of the feeding concentration depending on the cultivation. The digital control unit of the explosion-protected 15 L stirred tank reactor with 3 rushton turbines regulated the temperature at 30 °C, the pH at 6.8 and the stirrer speed at 500 rpm. All constants used in the model refer to values at 30 °C. The dissolved gas probes are from Mettler Toledo (InPro6800 and InPro5000i), the gas sensors are the BlueInOne Cell and BCP-H2 from BlueSens, the mass flow controllers and the pressure sensor are from Bronkhorst. Optical density (OD) was measured at 436 nm photometrically. Poly-β-3hydroxybutyrate (PHB) was isolated by digestion with sodium hypocholite as suggested by Jacquel N. et al. (2008). Phosphate is quantified photometrically with Phosphate FS* test-kit from DiaSys and the Berthelot-reaction described in Rhine et al. (1998) serves for ammonium determination.

3. CLOSED-LOOP CONTROL SCHEME

In microbial processes, growth and product formation depend on substrate concentrations and environmental conditions, e.g., pH. The latter, temperature, and foam level are held constant by basic controllers that are integrated in the control unit. The basic controllers calculate the flows of the correction fluids (u_{base}, u_{acid}, $u_{antifoam}$). Moreover, additional manipulating variables are the flow rates for liquid feedings (u_P, u_N, u_{Fe}) for phosphate (P), ammonium (N) and iron (Fe) with fixed feed concentrations (c_P, c_N, c_{Fe}). Figure 1 shows the control architecture of the process. The PI-controller for the gas phase receives the constant set point for the excess pressure (ΔP_{set})

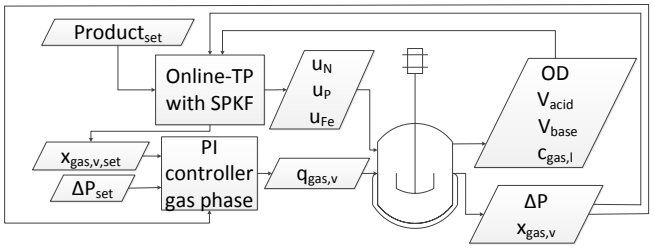

Fig. 1. Closed-loop control scheme for the autotrophic cultivation of *R. e.*

which is set to 40 mbar and the fractions for the gas phase composition ($x_{H_2,v,set}$, $x_{CO_2,v,set}$, $x_{O_2,v,set}$). It calculates the gas flows ($q_{H_2,v}$, $q_{CO_2,v}$, $q_{O_2,v}$) and regulates with it the gas phase composition in the headspace ($x_{H_2,v}$, $x_{CO_2,v}$, $x_{O_2,v}$) together with the excess pressure. The gas phase reference composition as well as the flow rates of the liquid feedings are determined with a model-based off-line or on-line trajectory planning (TP) aiming at maximum product in the end of the cultivation. On-line TP was the chosen model-based control variant, because it has advantages over tracking pre-computed set-points or set-trajectories as explained in Engell, S. (2007) and Heine et al. (2007). In every on-line TP step, the entire feeding-trajectories were calculated. A sigma-point Kalman filter for state estimation was employed. All manipulated variables are assembled in an input vector

$$\underline{u}^T = (u_N \quad u_{Fe} \quad u_P \quad q_{H_2,v} \quad q_{CO_2,v} \quad q_{O_2,v} \quad u_{base} \quad u_{acid} \quad u_{antifoam}). \tag{1}$$

4. MODEL

A rather detailed description of the model is given here as it has not been published before. The medium-sized structured, non-segregated model has three compartments which are biomass (X), the internal storage polymer poly-β-3hydroxybutyrate (PHB) and the membrane-bound hydrogenase (MBH). Gaseous substrates are hydrogen (H_2), carbon dioxide (CO_2), and oxygen (O_2). As limiting liquid substrates ammonium (N) and phosphate (P) will be considered. In the next paragraphs, balance equations for all states will be formulated before kinetic expressions for the reaction rates and measurement equations will be given.

4.1 State equations

The change of the amount of one component in a system is a result of the amount that comes into the system, the amount that leaves the system, and the amount that is generated or transformed in the system.
Accordingly, biomass (m_X) changes due to growth, which is determined by the growth rate (μ_X), and due to conversion of the storage molecule PHB into biomass, dictated by the rate $\mu_{X,PHB}$

$$\dot{m}_X = (Y_{N,X,PHB} + Y_{P,X,PHB} + 1) \cdot \mu_{X,PHB} \cdot m_X + \mu_X \cdot m_X. \tag{2}$$

This conversion comes with an uptake of phosphate and ammonium which is shown in the reaction

$$Y_{N,X,PHB} \cdot N + Y_{P,X,PHB} \cdot P + PHB \rightarrow X. \tag{3}$$

The conversion, as conventional growth, depends on the amount of active biomass (m_X) in (2).
The storage polymer PHB is built in proportion to biomass with the rate μ_{PHB} and degraded when converting it to biomass with the rate $\mu_{X,PHB}$

$$\dot{m}_{PHB} = \mu_{PHB} \cdot m_X - \mu_{X,PHB} \cdot m_X. \tag{4}$$

The amount of the target enzyme MBH (m_{MBH}) is balanced as well neglecting degradation

$$\dot{m}_{MBH} = \mu_{MBH} \cdot m_X. \tag{5}$$

The actual amount of MBH cannot be beasured but, in a certain reaction, the activity of the enzyme. It is assumed that this (relative) activity (a_{MBH}) is proportional to the mass of the enzyme

$$a_{MBH} = K_{MBH,a} \cdot m_{MBH}. \tag{6}$$

Details can be found in Rossner (2014). If (5) and (6) are combined,

$$\dot{a}_{MBH} = K_{MBH,a} \cdot \mu_{MBH} \cdot m_X \tag{7}$$

results.
In the reactor, the dissolved gas amounts see (8) to (10) for H_2, CO_2 and O_2 increase with the gas transfer into the medium ($\dot{m}_{tr,gas}$), and decrease because gas is consumed to produce biomass and PHB. The metabolic yield coefficients ($Y_{gas,X}$, $Y_{gas,PHB}$ and $Y_{gas,X,PHB}$) indicate how much gram of gas is required for one gram of biomass, for one gram of PHB and for the conversion of one gram PHB to biomass, respectively.

$$\begin{aligned}\dot{m}_{H_2,l} = &-(Y_{H_2,X,PHB} \cdot \mu_{X,PHB} + Y_{H_2,X} \cdot \mu_X + \\ &Y_{H_2,PHB} \cdot \mu_{PHB}) \cdot m_X + \dot{m}_{tr,H_2}\end{aligned} \tag{8}$$

$$\begin{aligned}\dot{m}_{CO_2,l} = &-(Y_{CO_2,X} \cdot \mu_X + Y_{CO_2,PHB} \cdot \mu_{PHB}) \cdot m_X \\ &+\dot{m}_{tr,CO_2}\end{aligned} \tag{9}$$

$$\begin{aligned}\dot{m}_{O_2,l} = &-(Y_{O_2,X,PHB} \cdot \mu_{X,PHB} + Y_{O_2,X} \cdot \mu_X + \\ &Y_{O_2,PHB} \cdot \mu_{PHB}) \cdot m_X + \dot{m}_{tr,O_2}\end{aligned} \tag{10}$$

The gas transfer rates are calculated exploiting the gas transfer coefficient (k_La) and Henry's law. Equation (11) describes the transport of a gas component (H_2, O_2 or CO_2) between the two phases

$$\dot{m}_{tr,gas} = k_L a_{gas} \cdot (c_{gas,sat} - c_{gas,l}) \cdot V_l \tag{11}$$

where k_La_{gas} is the volumetric gas transfer coefficient, $c_{gas,sat}$ the saturation concentration, $c_{gas,l}$ the concentration in the liquid phase, and V_l is the volume of the cultivation broth. The saturation concentration in the liquid phase is calculated by Henry's law,

$$c_{gas,sat} = Kh_{gas} \cdot p_{gas,v} \cdot M_{gas}, \tag{12}$$

with Kh_{gas} being the Henry coefficient, $p_{gas,v}$ the partial pressure in the gas phase, and M_{gas} the molar mass of the gas-component. The partial pressure is defined as

$$p_{gas,v} = x_{gas,v} \cdot P, \tag{13}$$

where $x_{gas,v}$ is the molar fraction and P the absolute pressure of the gas phase. The evaporation of water is also considered and discussed below.
Within the system, the micro-organisms consume ammonium for biomass production, MBH expression and the conversion of PHB to biomass which is given in (14). The corresponding yields are $Y_{N,X}$, $Y_{N,MBH}$ and $Y_{N,X,PHB}$, respectively. Besides the consumption terms, ammonium is also fed. The feed has an ammonium concentration of $c_{N,feed}$ and the feedrate is u_N.

$$\begin{aligned}\dot{m}_N = &-Y_{N,X,PHB} \cdot \mu_{X,PHB} \cdot m_X - Y_{N,X} \cdot \mu_X \cdot m_X - \\ &Y_{N,MBH} \cdot \dot{a}_{MBH} + u_N \cdot c_{N,feed}\end{aligned} \tag{14}$$

Similarly to the ammonium balance, the change of phosphate is described in (15).

$$\begin{aligned}\dot{m}_P = &-Y_{P,X,PHB} \cdot \mu_{X,PHB} \cdot m_X - Y_{P,X} \cdot \mu_X \cdot m_X - \\ &Y_{P,MBH} \cdot \dot{a}_{MBH} + u_P \cdot c_{P,feed}\end{aligned} \tag{15}$$

Equation (16) is the balance of acid compensated base to maintain a set-point pH of 6.8. During the cultivation, ammonium is bound by the organisms and that binding sets a proton free which lowers the pH in the cultivation broth. As the pH is feedback controlled with alkaline 3-molar NaOH, the consumption of one gram ammonium (N) can be converted into required volume of base (in mL) by dividing through $\frac{18\,\mathrm{g_N} \cdot 3\,\mathrm{mol_{OH^-}}}{\mathrm{mol_N} \cdot 1000\,\mathrm{mL}}$ (see (16)). As dissolving or gassing out of CO_2 has a pH-effect as well, a third term has to be included in (16).

$$\begin{aligned}\dot{V}_{BaAc} = &\frac{(Y_{N,X} \cdot \mu_X + Y_{N,X,PHB} \cdot \mu_{X,PHB}) \cdot m_X}{18 \frac{\mathrm{g_N}}{\mathrm{mol_N}} \cdot \frac{3\,\mathrm{mol_{OH^-}}}{1000\,\mathrm{mL}}} + \\ &\frac{Y_{N,MBH} \cdot \dot{a}_{MBH}}{18 \frac{\mathrm{g_N}}{\mathrm{mol_N}} \cdot \frac{3\,\mathrm{mol_{OH^-}}}{1000\,\mathrm{mL}}} + \\ &K_{BaAc,pCO_2} \cdot \dot{m}_{CO_2,l} \cdot 1000 \frac{\mathrm{mg}}{\mathrm{g}}\end{aligned} \tag{16}$$

The volume of the cultivation changes over time because of liquid substrate feeding (u_i) and correction fluids. Moreover, water evaporates into the system headspace and is transferred out of the system with a defined outlet stream ($\dot{m}_{H_2O,out}$) that is directed to the gas sensors. Furthermore, *R. e.* produces water in the energy metabolism. That impact is considered with yield factors $Y_{H_2O,PHB}$=$Y_{H_2O,X,PHB}$=6.25g·g^{-1}, $Y_{H_2O,X}$=3.47g·g^{-1} in (17) which are calculated from stoichiometric reaction equations (not shown here). The volume balance finally reads

$$\begin{aligned}\dot{V}_l = &\frac{1}{\rho_{H_2O}} \cdot Y_{H_2O,PHB} \cdot (\mu_{PHB} + \mu_{X,PHB}) \cdot m_X + \\ &\frac{1}{\rho_{H_2O}} \cdot (Y_{H_2O,X} \cdot \mu_X \cdot m_X - \dot{m}_{H_2O,out}) + \\ &u_{antifoam} + u_{acid} + u_{base} + u_N + u_{Fe} + u_P.\end{aligned} \tag{17}$$

Moreover, the volume and other states are affected by sampling. Therefore, the effect of sampling is accounted for as well in the model. The states are assembled in a vector

$$\begin{aligned}\underline{x}^T = (&m_X \;\; m_{PHB} \;\; a_{MBH} \;\; m_{H_2,l} \\ &m_{CO_2,l} \;\; m_{O_2,l} \;\; m_N \;\; m_P \;\; V_{BaAc} \;\; V_l)\end{aligned} \tag{18}$$

Table 2. Kinetic functions used in the model. Each kinetic function g(c) depends on the substrate concentrations c and the constant parameters k that have to be identified.

Notation	Type	Kinetic function $g(c)$	Standardisation term g_{max}^{-1}
$\mathrm{MiMe}(c,k)$	lim	$\frac{c}{c+k}$	-
$\mathrm{Ai}(c,k)$	in	e^{-kc}	-
$\mathrm{Spec}_1(c,k)$	lim, in	$\frac{g_{max}^{-1}\cdot c}{1+c+\left(\frac{c}{k}\right)^2}$	$1+\frac{2}{k}$
$\mathrm{Spec}_2(c,k_1\ k_2)$	lim, in	$\frac{g_{max}^{-1}\cdot c}{1+c+\left(\frac{c}{k_1}\right)^{k_2}}$	$1+\frac{k_2(k_2-1)^{\frac{1}{k_2}}}{(k_2-1)k_1}$
$\mathrm{Spec}_3(c_1\ c_2,k_1\ k_2)$	in	$\max(e^{-k_1\cdot c_1}, e^{-k_2\cdot c_2})$	-

4.2 Kinetics

Any kind of production rate in chemical and biochemical reactions depends on the availability of the substrates and the exposure to inhibitors. Those biochemical dependencies are described in various kinetic equations. The ones used in this model are introduced in Tab. 2. The Michaelis-Menten (MiMe) kinetic describes growth on a limiting (lim) substrate (Michaelis and Menten, 1913). An inhibiting (in) dependency on a single substrate is expressed by the Aiba (Ai) kinetic (Aiba et al., 1968). Limiting effects on growth at low concentrations followed by inhibition at high substrate amounts (lim, in) are realized with a special function, Spec_1, which employs one parameter and Spec_2 with two parameters taken from Rossner (2014). Additionally, a new kinetic named Spec_3 is used which describes the inhibitory effects of two substrates on growth.

Biomass production. The growth rate (μ_X) for the PHB-free biomass depends on the concentrations of substrates required for growth and on the presence of inhibitors. Substrates for growth are ammonium, phosphate, trace elements, CO_2, O_2, and H_2. Trace elements are assumed to be present in sufficient amounts at all times and, therefore, are not effecting growth. Hydrogen has a positive effect on the growth rate. The more hydrogen is available, the higher the growth rate is. This relation is described by a Michaelis-Menten kinetic $\mathrm{MiMe}(c_{H_2,l}, k_{H_2}^X)$. The ammonium and phosphate dependencies are implemented by Michaelis-Menten kinetics as well, $(\mathrm{MiMe}(c_N, k_N^X), \mathrm{MiMe}(c_P, k_P^X))$. It is assumed that high salt concentrations inhibit growth but in our cultivations with ammonium concentrations up to 8 $\mathrm{g{\cdot}L^{-1}}$ and phosphate up to 5.5 $\mathrm{g{\cdot}L^{-1}}$ this inhibition was not observed. Therefore, MiMe is used and we set constraints on high salt concentrations when optimising. Carbon dioxide and oxygen are also substrates. Oxygen as the electron acceptor is involved in energy production and carbon dioxide is fixed anabolically. The presence of both gases is required for growth. On the other hand, high oxygen concentrations are known to inhibit the activity of the hydrogenases that are directly involved in the energy production cycle (Ludwig et al., 2009). Inhibitory effects on growth at high concentrations have been described by Shang et al. (2003) for carbon dioxide as well. Therefore, the kinetics for these gases follow the bell curve of an inhibition. The kinetic of choice for the substrate oxygen is the 2-parametric special function ($\mathrm{Spec}_2(c_{O_2,l}, k_{1,O_2}^X\ k_{2,O_2}^X)$). For CO_2 the 1-parametric function $\mathrm{Spec}_1(c_{CO_2,l}, k_{CO_2}^X)$ was selected. As a result, the growth rate is described by

$$\begin{aligned}\mu_X = \mu_{max,X} \cdot \mathrm{MiMe}(c_N, k_N^X) \cdot \mathrm{MiMe}(c_P, k_P^X) \cdot \\ \mathrm{MiMe}(c_{H_2,l}, k_{H_2}^X) \cdot \mathrm{Spec}_2(c_{O_2,l}, k_{1,O_2}^X\ k_{2,O_2}^X) \cdot \\ \mathrm{Spec}_1(c_{CO_2,l}, k_{CO_2}^X). \end{aligned} \quad (19)$$

The parameter $\mu_{max,X}$ in (19) is the maximum biomass production rate.

PHB production and degradation. It is known that in autrotrophic cultivations the production of the storage polymer PHB increases when phosphate and/or ammonium limitation occurs as mentioned by Repaske and Repaske (1976) and Ryu et al. (1997). For the PHB production rate μ_{PHB}, this relation is described by an Aiba kinetic. Likewise, the PHB concentration itself effects the formation of PHB. The higher the PHB fraction of the overall biomass is ($x_{PHB,X}{=}c_{PHB}{\cdot}\ (c_X{+}c_{PHB})^{-1}$), the less PHB is produced. This inhibitory effect is also implemented with an Aiba term. Similar to the biomass production, all three gases are required for the assimilation of PHB. In autotrophic metabolism, all carbon present in the cell is primarily fixed through the Calvin-Benson-Bassham (CBB) pathway (Park et al., 2011) and then either processed to biomass or to the storage polymer PHB. It is assumed that the CBB pathway is the velocity-limiting step for carbon assimilation. Therefore, the kinetics for the PHB production rate concerning the gases are implemented identically to those for the growth rate.

$$\begin{aligned}\mu_{PHB} = \mu_{max,PHB} \cdot \mathrm{Spec}_3(c_N\ c_P, k_N^{PHB}\ k_P^{PHB}) \cdot \\ \mathrm{MiMe}(c_{H_2,l}, k_{H_2}^X) \cdot \mathrm{Spec}_2(c_{O_2,l}, k_{1,O_2}^X\ k_{2,O_2}^X) \cdot \\ \mathrm{Ro}_1(c_{CO_2,l}, k_{CO_2}^X) \cdot \mathrm{Ai}(x_{PHB,X}, k_{PHB}^{PHB}) \end{aligned} \quad (20)$$

Assimilated PHB is converted to biomass as suggested by Schlegel et al. (1961) and Bartha (1962). In the model it is implemented with the conversion rate $\mu_{X,PHB}$. The conversion takes place when the substrate carbon dioxide is missing and ammonium as well as phosphate are present. This dependency is described by an Aiba kinetic on carbon dioxide, and Michaelis-Menten kinetic for phosphate and ammonium which are, for simplicity, identical to those describing biomass production. PHB needs to be present in significant amounts for that conversion which is implemented by a MiMe kinetic term for the present fraction of PHB ($x_{PHB,X}$).

$$\begin{aligned}\mu_{X,PHB} = \mu_{max,X,PHB} \cdot \mathrm{Ai}(c_{CO_2,l}, k_{CO_2}^{X,PHB}) \cdot \\ \mathrm{MiMe}(c_N, k_N^X) \cdot \mathrm{MiMe}(c_P, k_P^X) \cdot \\ \mathrm{MiMe}(x_{PHB,X}, k_{PHB}^{X,PHB}) \end{aligned} \quad (21)$$

MBH expression. It is assumed that the driving force for the expression of membrane bound hydrogenase (MBH) is given by the difference between the possible MBH amount due to current hydrogen availability ($m_{MBH,sat}$) and the MBH amount that is present m_{MBH}.

$$\mu_{MBH} = \mu_{max,MBH} \cdot (m_{MBH,sat} - m_{MBH}) \quad (22)$$

Multiplying this equation with $K_{MBH,a}$ gives an expression in the activities.

$$K_{MBH,a} \cdot \mu_{MBH} = \mu_{max,MBH} \cdot (a_{MBH,sat} - a_{MBH}) . \quad (23)$$

The theoretically possible amount of MBH is calculated by Rossner (2014) with

$$a_{MBH,sat} = (a_{MBH,max} - a_{MBH,min}) \cdot \mathrm{Ai}(c_{H_2,l}, k_{H_2}^{MBH}) + a_{MBH,min}. \quad (24)$$

The model assumes a minimal MBH amount at high hydrogen concentrations ($m_{MBH,min}$). The MBH amount at low hydrogen concentrations is limited due to the nature of the cell membrane ($m_{MBH,max}$). All amounts between those limits depend on the hydrogen concentration. The lower the concentration, the higher the MBH expression. That relation follows an Aiba kinetic with the parameter $k_{H_2}^{MBH}$ to be identified.

4.3 Measurement equations

In order to compare the model with real data, measurement equations have to be defined that describe the relationships between the state variables and the measured variables. Furthermore, inputs calculated by the gas controller are used as well. Due to the analytic process in the laboratory, the biomass concentration that is measured is always the sum of the PHB-free cells (m_X) and internal PHB (m_{PHB}) divided by the volume (V_l) as shown in (25). The optical density (OD), measured photometrically at 436 nm, is proportional to the sum of the PHB-free biomass concentration multiplied by a factor $K_{OD,X}$ and the PHB concentration multiplied by $K_{OD,PHB}$ see (26). Equations (27) to (29) represent the measured concentrations of the gas components in the fermenter outlet ($x_{H_2,v}$, $x_{CO_2,v}$, $x_{O_2,v}$). For the excess pressure (ΔP) in mbar given in (30), the environmental pressure P_0 in Pa is subtracted from the measured pressure P in the system and divided by 100 Pa·mbar^{-1}. Measurement equations (31) to (33) express the volumetric flow rates of each gas component (q_{H_2}, q_{CO_2}, q_{O_2}) in L·h^{-1}. Each of them equal the sum of the defined outlet ($\dot{m}_{gas,out}$) and the gas amount which is transferred into the liquid phase ($\dot{m}_{tr,gas}$) divided by the environmental pressure and the molar mass and multiplied with the ideal gas constant (R), the room temperature (T) and a conversion factor. The amount of gas needed for MBH is very small and therefore not taken into account. The ammonium and phosphate concentrations (c_N, c_P) are given in (34) and (35). The dissolved CO_2 concentration in mg·L^{-1} is calculated in (36) by multiplying the dissolved carbon dioxide concentration ($m_{CO_2,l} \cdot V_l^{-1}$) with a conversion factor. Dissolved oxygen is measured in %. Therefore, the dissolved O_2-concentration ($m_{O_2,l} \cdot V_l^{-1}$) is divided by the maximum concentration at that pressure and temperature ($c_{O_2,sat,air}$) which is calculated according to Henry's law. The volume of acid compensated base (V_{BaAc}) is given by (38). In the parameter identification step it is compared to the difference of the transferred volumes of the base and acid feedings. The next measurement equation (39) is the specific activity of MBH. Finally, the concentration of PHB (c_{PHB}) in (40) is given and the volume (V_l) in (41).

$$y_1 = \frac{m_X + m_{PHB}}{V_l} \quad (25)$$

$$y_2 = K_{OD,X} \cdot \frac{m_X}{V_l} + K_{OD,PHB} \cdot \frac{m_{PHB}}{V_l} \quad (26)$$

$$y_3 = x_{H_2,v} \quad (27)$$

$$y_4 = x_{CO_2,v} \quad (28)$$

$$y_5 = x_{O_2,v} \quad (29)$$

$$y_6 = \frac{P - P_0}{100 \frac{\mathrm{Pa}}{\mathrm{mbar}}} \quad (30)$$

$$y_7 = \frac{(\dot{m}_{H_2,out} + \dot{m}_{tr,H_2})}{M_{H_2} \cdot P_0} \cdot R \cdot T \cdot 10^3 \frac{\mathrm{L}}{\mathrm{m}^3} \quad (31)$$

$$y_8 = \frac{(\dot{m}_{CO_2,out} + \dot{m}_{tr,CO_2})}{M_{CO_2} \cdot P_0} \cdot R \cdot T \cdot 10^3 \frac{\mathrm{L}}{\mathrm{m}^3} \quad (32)$$

$$y_9 = \frac{(\dot{m}_{O_2,out} + \dot{m}_{tr,O_2})}{M_{O_2} \cdot P_0} R \cdot T \cdot 10^3 \frac{\mathrm{L}}{\mathrm{m}^3} \quad (33)$$

$$y_{10} = \frac{m_N}{V_l} \quad (34)$$

$$y_{11} = \frac{m_P}{V_l} \quad (35)$$

$$y_{12} = \frac{m_{CO_2,l}}{V_l} \cdot 1000 \frac{\mathrm{mg}}{\mathrm{g}} \quad (36)$$

$$y_{13} = \frac{\frac{m_{O_2,l}}{V_l} \cdot 100\,\%}{c_{o2,sat,air}} \quad (37)$$

$$y_{14} = V_{BaAc} \quad (38)$$

$$y_{15} = a_{MBH} \quad (39)$$

$$y_{16} = \frac{m_{PHB}}{V_l} \quad (40)$$

$$y_{17} = V_l \quad (41)$$

4.4 Parameters

Some parameters were determined by separate experiments or taken from theoretical evaluations from literature. As given in (26), the OD is described by a combination of linear expressions depending on the biomass and PHB concentrations. The parameters ($K_{OD,X}$ and $K_{OD,PHB}$) were calculated by multiple linear regression using a least square approach. The regression leads to values of 5.41 g·L^{-1} and 13.09 g·L^{-1} for the parameters $K_{OD,X}$ and $K_{OD,PHB}$, respectively. The relative standard deviation is 5.3 % for $K_{OD,X}$ and 9.2 % for the parameter $K_{OD,PHB}$.
The initial value of the volumetric gas transfer rate (k_La) for oxygen was determined experimentally by Rossner (2014) and validated with extra experiments (not shown). The k_La value of carbon dioxide was also determined at first by extra experiments and the k_La value for hydrogen was calculated according to the film theory explained in Garcia-Ochoa and Gomez (2009). The initial values of the yield coefficients were take from Bongers (1970), Morinaga et al. (1978) and Tanaka et al. (1995).
All parameters shown in Tab. 3 were estimated with the data of 15 cultivations where PHB was measured only in three of the 15. Few measurements explain the comparatively high relative standard deviations for some of the

parameters belonging to PHB description. Additionally to the 15 identification experiments, four cultivations served for validation. Two exemplary cultivations used for identification are shown in Fig. 2 and 3 where the simulations are compared to the measurements. In the cultivation of Fig. 2, slow growth is caused by high dissolved oxygen concentrations. In the identified experiment shown in Fig. 3, fast growth is triggered by low oxygen concentrations at first. That growth stage is followed by a high expression of MBH due to low specific hydrogen concentrations. This observation confirms the statement by Friedrich et al. (1981) that deficiency of electrons enhances the expression of MBH.

Table 3. Estimated parameter values, allowed interval [min, max] and relative standard deviation (rel. std d.) in % calculated with Fisher analysis

Name	Unit	Value	[min, max]	rel. std d.
K_{BaAc,pCO_2}	$mL \cdot mg^{-1}$	0.04	[0.016, 0.2]	0.21
$k_L a_{H_2}$	h^{-1}	272	[30, 900]	0.04
$k_L a_{CO_2}$	h^{-1}	38	[0.2, 580]	0.08
$k_L a_{O_2}$	h^{-1}	193	[150, 800]	0.05
$Y_{N,X}$	$g \cdot g_X^{-1}$	0.18	[0.08, 0.3]	0.05
$Y_{P,X}$	$g \cdot g_X^{-1}$	0.08	[0.004, 0.3]	0.03
$Y_{H_2,X}$	$g \cdot g_X^{-1}$	0.4	[0.3, 0.71]	0.05
$Y_{CO_2,X}$	$g \cdot g_X^{-1}$	1.36	[1.32, 3.96]	0.07
$Y_{O_2,X}$	$g \cdot g_X^{-1}$	1.62	[1.6, 0.84]	0.06
$Y_{N,X,PHB}$	$g \cdot g_{PHB}^{-1}$	0.69	[0.01, 4]	0.37
$Y_{P,X,PHB}$	$g \cdot g_{PHB}^{-1}$	0.46	[0.02, 2]	0.47
$Y_{H_2,X,PHB}$	$g \cdot g_{PHB}^{-1}$	1.28	[0.2, 1.8]	0.42
$Y_{O_2,X,PHB}$	$g \cdot g_{PHB}^{-1}$	0.48	[0.1, 1.5]	0.36
$Y_{H_2,PHB}$	$g \cdot g_{PHB}^{-1}$	0.45	[0.2, 0.73]	0.19
$Y_{CO_2,PHB}$	$g \cdot g_{PHB}^{-1}$	2.9	[1.32, 5.28]	0.13
$Y_{O_2,PHB}$	$g \cdot g_{PHB}^{-1}$	1.71	[1.28, 6.4]	0.13
$Y_{N,MBH}$	$g \cdot mg_{MP} U^{-1}$	3.9e-3	[0, 0.5]	8.98
$\mu_{max,X}$	h^{-1}	0.35	[0.1, 0.7]	0.05
$k_{H_2}^X$	$mg \cdot L^{-1}$	4e-3	[2e-4, 0.61]	2.68
$k_{CO_2}^X$	$mg \cdot L^{-1}$	44.59	[4.4, 176]	0.02
k_{1,O_2}^X	$mg \cdot L^{-1}$	1.62	[1.6, 2.56]	0.08
k_{2,O_2}^X	-	2.140	[2, 8]	0.04
k_N^X	$g \cdot L^{-1}$	0.34	[0.1, 0.8]	0.15
k_P^X	$g \cdot L^{-1}$	0.72	[0.4, 1.5]	0.08
$\mu_{max,X,PHB}$	h^{-1}	0.2	[0.1, 2.7]	15.58
$k_{CO_2}^{X,PHB}$	$L \cdot mg^{-1}$	782	[88, 1980]	1.41
$k_{PHB}^{X,PHB}$	-	9.96	[0.01, 10]	16.17
$\mu_{max,PHB}$	h^{-1}	0.11	[0, 0.85]	0.28
k_P^{PHB}	$L \cdot g^{-1}$	80	[1, 100]	0.23
k_N^{PHB}	$L \cdot g^{-1}$	1.79	[0.2, 20]	0.35
k_{PHB}^{PHB}	-	2	[0.1, 3.1]	0.28
$\mu_{max,MBH}$	h^{-1}	2.8e-3	[2.e-3, 0.01]	0.65
$a_{MBH,min}$	$U \cdot mg_{MP}^{-1}$	0.46	[0.1, 0.6]	5.84
$a_{MBH,max}$	$U \cdot mg_{MP}^{-1}$	6.87	[5, 15]	0.36
$k_{H_2}^{MBH}$	$L \cdot mg^{-1}$	1.89	[0.99, 2.47]	1.11

5. MODEL BASED CONTROL AND VALIDATION

The overall aim of this work was to set up a control system that includes on-line TP to maximise the amount of biomass and PHB in an autotrophic cultivation of *R. e.*. Figure 4 shows a cultivation where an on-line TP was used between t=22 h and t=120 h. It ended before the cultivation was finished, because from t=120 h onwards the degradation of PHB was investigated and at that time the model did not describe the PHB conversion pathway to a sufficient extend. The data of the cultivation shown in Fig. 4 for t>120 h were used to identify all parameters involved in PHB degradation more accurately. The resulting parameter values and their standard deviations are also listed in Tab. 3. With the identified parameter set, the simulated degradation reveals the measurements which is compared Fig. 4, t>120 h.

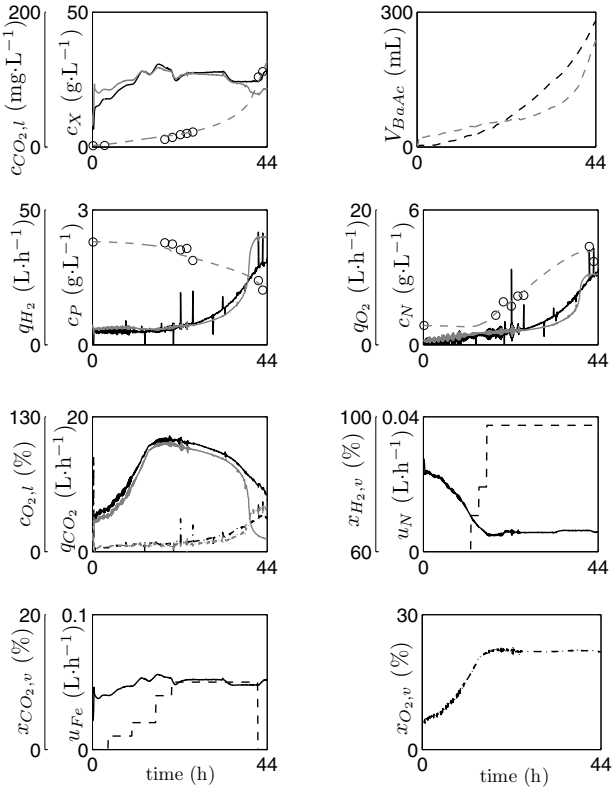

Fig. 2. Exemplary cultivation result for parameter identification. Simulations are given in grey and measurements in black. Solid lines refer to the outer axis and dotted lines/circles to the inner axis. Optical density (OD), ammonium (N) and phosphate (P) as well as volume flow of carbon dioxide (q_{CO_2}) and flow rates (u) for ammonium and iron (Fe) are plotted on the inner axis. The last three plots are the liquid feed rates and the gas fractions in the headspace.

The feeding trajectories in the cultivation were calculated on-line and were allowed to be changed every 10 hours. During the entire cultivation, the SPKF state estimation algorithm, was running. The estimated non-measurable states served as start vectors for the on-line optimisation. The aim was to increase the biomass concentration until t=50 h and for t=50–120 h to maximise the PHB amount due to phosphate limitation. The data up to t=50 h were not used for identification and represent an exemplary validation experiment.

In Fig. 5 the results of an off-line trajectory planning (TP) are compared to the on-line TP results. The feeding profiles are shown. All feeds were allowed to be changed every 10 hours. Changes in the gas composition were realised as ramps and changes in the liquid ammonium feed as steps. Comparing the off-line with the on-line trajectories, it is notable that the on-line optimiser calculated a higher feed for ammonium at t=50 h. This was a reaction towards the decrease of ammonium concentration which was estimated by the SPKF. Ammonium concentrations below 1 g·L^{-1} were not allowed by constraints during the optimisation. This constraint was set because low ammonium concentrations also lead to PHB production, but only the impact of phosphate depletion on the PHB formation was to be investigated in this run.

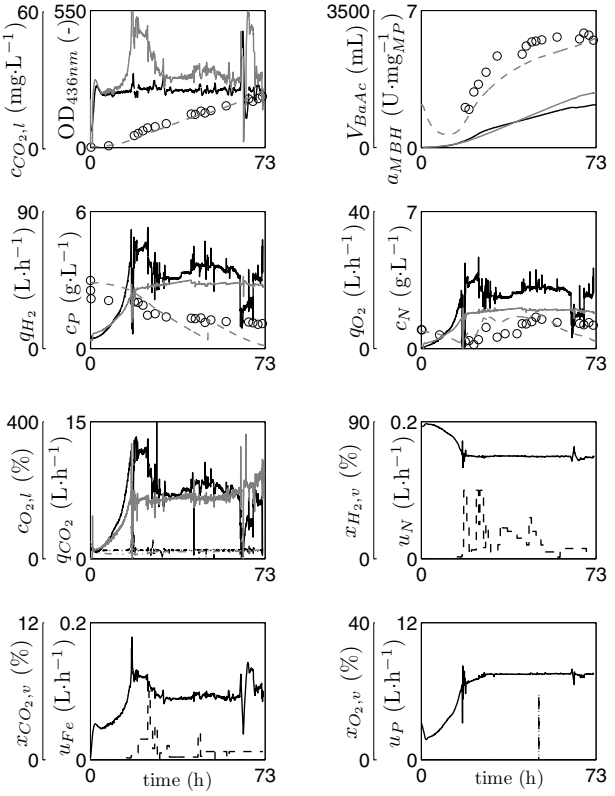

Fig. 3. Exemplary cultivation result for parameter identification. For more details see Fig. 2. Additionally, the specific activity a_{MBH} is shown in the second plot.

The on-line optimisation (see Fig. 5) also lowered the hydrogen fraction in the gas phase and increased the carbon dioxide amount between t=22 h and t=36 h. At first sight, considering the kinetics used in μ_X and μ_{PHB}, this result seems to be counterproductive to biomass growth and production of PHB. But when running a process robustly, short deficiencies of substrate can be beneficial because then the required concentration can be adjusted more accurately. That has been shown in simulation studies in Kawohl et al. (2007). It can be concluded that the hydrogen limitation did not effect the metabolisms described in the model because the model reflects the process even after the limitation (t>36 h) as shown in Fig. 4.

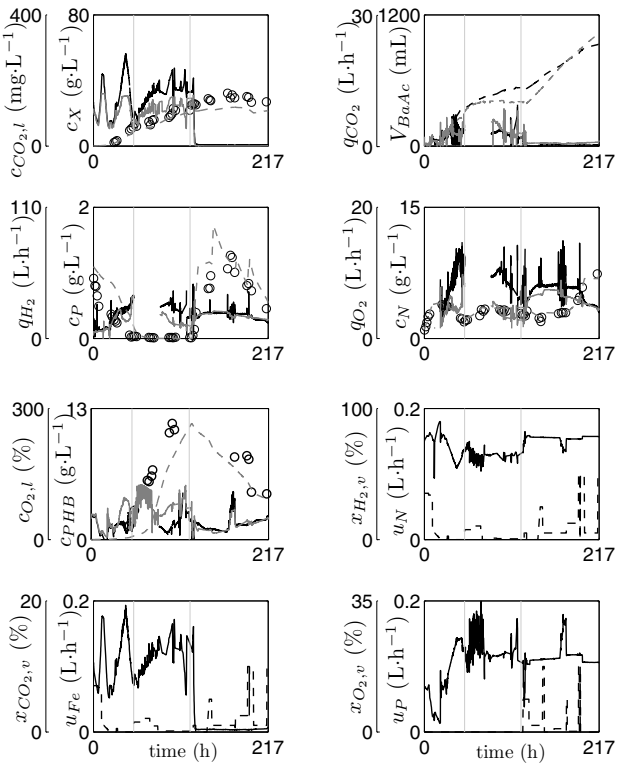

Fig. 4. Cultivation run with on-line TP. Measurements (black) are compared to the post-experimental simulations (grey). For details to indices see caption of Fig. 2. The aim was to maximise the biomass (c_X) and PHB (c_{PHB}) concentration induced by phosphate limitation until t=50 h and t=120 h, respectively. These time instants are given in light grey, vertical lines. All measurements shown here that are not plottet in circles plus the OD were used for state estimation. The data of q_{gas} and $c_{O_2,l}$ between t=50 h and t=85 h are inconclusive caused by pressure fluctuations and therefore not shown.

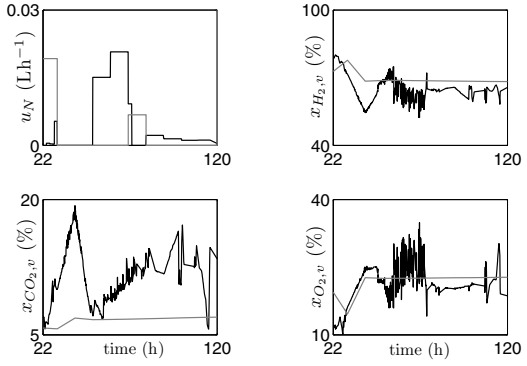

Fig. 5. Comparison between off-line (grey) optimised feed trajectories and on-line optimised (black) development of gaseous and ammonium feed with the aim to maximise the biomass concentration and the PHB production due to phosphate limitation.

6. CONCLUSION

A model for the autotrophic cultivation of *R. e.* was set up and exploited in a model-based closed-loop control with the aim to maximise the amount of active biomass or internal storage compound PHB. It can also be used for the optimised production of membrane bound hydrogenase, but the results are not shown here. By on-line optimisation, the feedings and consequently the substrate concentrations were adjusted, leading to fast growth and PHB production.
The model is sufficient for our purposes and the parameters involved in biomass, PHB and MBH production have been estimated satisfactorily.
In the future, we will work on a model extension to describe and control the formation of soluble hydrogenase (SH), that is currently in the focus of research (Lauterbach et al. (2011), Burgdorf et al. (2005)).

REFERENCES

Aiba, S., Shoda, M., and Nagatani, M. (1968). Kinetics of product inhibition in alcohol fermentation. *Biotechnol. Bioeng.*, 10, 845–864.

Bartha, R. (1962). Physiologische untersuchungen über den chemolithotrophen stoffwechsel neu isolierter hydrogenomonas-stämme. *Archiv für Mikrobiologie*, 41(3), 313–350.

Bongers, L. (1970). Energy generation and utilization in hydrogen bacteria. *J. Bacteriol.*, 104(1), 145–151.

Burgdorf, T., Lenz, O., Buhrke, T., van der Linden, E., Jones, A.K., Albracht, S.P., and Friedrich, B. (2005). [nife]-hydrogenases of ralstonia eutropha h16: modular enzymes for oxygen-tolerant biological hydrogen oxidation. *J. Mol. Microbiol. Biotechnol.*, 10(2-4), 181–196.

Engell, S. (2007). Feedback control for optimal process operation. *J. Process Control*, 17(3), 203–219.

Friedrich, C.G., Friedrich, B., and Bowien, B. (1981). Formation of enzymes of autotrophic metabolism during heterotrophic growth of alcaligenes eutrophus. *J. Gen. Microbiol.*, 122(1), 69–78.

Garcia-Ochoa, F. and Gomez, E. (2009). Bioreactor scale-up and oxygen transfer rate in microbial processes: an overview. *Biotechnol. Adv.*, 27(2), 153–176.

Heine, T., Kawohl, M., and King, R. (2007). Model based estimation and optimal control of fed-batch fermentation processes for the production of antibiotics. *Chem. Eng. Process.*, 1223–1241.

Jacquel N., Lo C.-W., Wei Y.-H., Wu H.-S., and Wang S. S. (2008). Isolation and purification of bacterial poly(3-hydroxyalkanoates). *Biochem. Eng. J.*, 39(1), 15–27.

Kawohl, M., Heine, T., and King, R. (2007). A new approach for robust model predictive control of biological production processes. *Chem. Eng. Sci.*, 62(18–20), 5212–5215.

King, R. (1997). A structured mathematical model for a class of organisms: I. development of a model for streptomyces tendae and application of model-based control. *J Biotech*, 52(3), 219–234.

Lauterbach, L., Liu, J., Horch, M., Hummel, P., Schwarze, A., Haumann, M., Vincent, K.A., Lenz, O., and Zebger, I. (2011). The hydrogenase subcomplex of the nad+-reducing [nife] hydrogenase from ralstonia eutropha – insights into catalysis and redox interconversions. *Eur. J. Inorg. Chem.*, 2011(7), 1067–1079.

Ludwig, M., Cracknell, J.A., Vincent, K.A., Armstrong, F.A., and Lenz, O. (2009). Oxygen-tolerant h2 oxidation by membrane-bound [nife] hydrogenases of ralstonia species. coping with low level h2 in air. *J. Biol. Chem.*, 284(1), 465–477.

Mandenius, C.F. and Titchener-Hooker, N.J. (eds.) (2013). *Measurement, Monitoring, Modelling and Control of Bioprocesses*. Adv. Biochem. Engin./Biotechnol. Springer Berlin Heidelberg.

Michaelis, L. and Menten, M.L. (1913). Die kinetik der invertinwirkung. *Biochem. Z.*, 49, 334–369.

Morinaga, Y., Yamanaka, S., Ishizaki, A., and Hirose, Y. (1978). Growth characteristics and cell composition of alcaligenes eutrophus in chemostat cultures. *Agric. Biol. Chem.*, 42, 439–444.

Park, J., Kim, T., and Lee, S. (2011). Genome-scale reconstruction and in silico analysis of the ralstonia eutropha h16 for polyhydroxyalkanoate synthesis, lithoautotrophic growth, and 2-methyl citric acid production. *BMC Syst Biol*, 5(1), 101.

Repaske, R. and Repaske, A.C. (1976). Quantitative requirements for exponential growth of alcaligenes eutrophus. *Appl. Environ. Microbiol.*, 32(4), 585–591.

Rhine, E.D., Mulvaney, R.L., Pratt, E.J., and Sims, G.K. (1998). Improving the berthelot reaction for determining ammonium in soil extracts and water. *Soil Sci Am J*, (62), 473–480.

Rossner, N. (2014). *Robuste modellbasierte Prozessführung auf Basis von Gaußschen Mischdichten am Beispiel der Bray-Liebhafsky-Reaktion und der autotrophen Kultivierung von Ralstonia eutropha H16*. Ph.D. thesis, Technische Universität Berlin, Berlin.

Ryu, H.W., Hahn, S.K., Chang, Y.K., and Chang, H.N. (1997). Production of poly(3-hydroxybutyrate) by high cell density fed-batch culture of alcaligenes eutrophus with phospate limitation. *Biotechnol. Bioeng.*, 55(1), 28–32.

Schlegel, H.G., Gottschalk, G., and Bartha, R. (1961). Formation and utilization of poly-beta-hydroxybutyric acid by knallgas bacteria (hydrogenomonas). *Nature*, 191, 463–465.

Shang, L., Jiang, M., Ryu, C.H., Chang, H.N., Cho, S.H., and Lee, J.W. (2003). Inhibitory effect of carbon dioxide on the fed-batch culture of ralstonia eutropha: Evaluation by co2 pulse injection and autogenous co2 methods. *Biotechnol. Bioeng.*, 83(3), 312–320.

Tanaka, K., Ishizaki, A., Kanamaru, T., and Kawano, T. (1995). Production of poly(d-3-hydroxybutyrate) from co2, h2, and o2 by high cell density autotrophic cultivation of alcaligenes eutrophus. *Biotechnol. Bioeng.*, 45(3), 268–275.

Waldraff, W., Biener, R., Oswald, G., Sippel, G., King, R., and Gilles, E.D. (1993). Model-based control of bioprocesses - trajectory optimization and control. In Schmid (ed.), *Biochemical Engineering*, volume 3 of *Biochemical Engineering*, 171–173. Verlag Kurz & Co.

Waldraff, W., King, R., and Gilles, E.D. (1997). Optimal feeding strategies by adaptive mesh selection for fed-batch bioprocesses. *Bioprocess Eng.*, 17(4), 221–227.

